[CANCER RESEARCH 64, 3436–3443, May 15, 2004]

Perturbed IFN-γ-Jak-Signal Transducers and Activators of Transcription Signaling in Tuberous Sclerosis Mouse Models: Synergistic Effects of Rapamycin-IFN-γ Treatment

Nisreen El-Hashemite, Hongbing Zhang, Victoria Walker, Karin M. Hoffmeister, and David J. Kwiatkowski

Brigham and Women's Hospital, Hematology Division, Department of Medicine, Harvard Medical School, Boston, Massachusetts

ABSTRACT

Tuberous sclerosis complex (TSC) is an autosomal dominant disorder characterized by widespread development of hamartomas, which is caused by mutations in either *TSC1* or *TSC2*. We demonstrate a dramatic decrease of IFN-γ expression in tumors and mouse embryo fibroblast cell lines that lack either Tsc1 or Tsc2, which is reversed by rapamycin (mammalian target of rapamycin inhibitor) therapy. Increased signal transducers and activators of transcription (STAT) 1 expression and phosphorylation at Ser 727 and increased pSTAT3 Tyr705 levels also are seen in Tsc1 null and Tsc2 null cells and in tumors. Treatment of Tsc1 or Tsc2 null cells with IFN-γ induces apoptosis, in contrast to control cell lines, with reduction in pSTAT3 Tyr705 levels and major increases in pSTAT1 Tyr701, bax, and caspase-1 and -9 levels. A combination of IFN-γ and rapamycin is markedly synergistic in induction of apoptosis in Tsc1 or Tsc2 null cells because pSTAT3 Tyr705 phosphorylation is abolished completely and the other effects of IFN-γ are maintained or enhanced. Rapamycin-IFN-γ has unique potential therapeutic benefit for management of TSC tumors.

INTRODUCTION

Tuberous sclerosis complex (TSC) is an autosomal dominant genetic disorder characterized by multiorgan hamartomatosis as a result of mutations in either *TSC1* or *TSC2* (1). TSC1 and TSC2 form a protein complex (2, 3), and mutations in either gene lead to similar clinical phenotypes, which are somewhat more severe for *TSC2* mutations (4, 5). TSC follows the two-hit model of tumor suppressor genes because TSC lesions often show loss of heterozygosity for the wild-type allele corresponding to the germline mutation in either *TSC1* or *TSC2* (6). We and others have reported that loss of either *TSC* gene results in unregulated activation of mammalian target of rapamycin (mTOR), which leads to activation and phosphorylation of S6K and S6, in cultured cell lines, patient TSC lesions, and Tsc mouse model tumors (7–11). This activation is highly sensitive to rapamycin (mTOR inhibitor) therapy. The mechanism of activation of mTOR in the absence of either TSC1 or TSC2 has been related recently to loss of the GTPase-activating protein activity of the TSC2 protein for the Rheb GTPase (12–15). Rheb-GTP appears to be a major positive regulator of mTOR activity.

We have shown recently that deficiency in either Tsc1 or Tsc2 results in a marked increase in vascular endothelial growth factor (VEGF; a potent angiogenic factor) production *in vitro* and *in vivo*, which also is sensitive to rapamycin therapy (16). Rapamycin is clinically approved for the prevention of allograft rejection and exerts its effects by binding to the cyclophilin FKBP12, which then binds to and inhibits mTOR (17, 18). Therefore, rapamycin is a promising therapeutic agent for TSC hamartomas.

We also have observed an association between an IFN-γ allele that is associated with higher secretion of IFN-γ and a milder clinical phenotype of TSC renal angiomyolipoma (19). Angiomyolipomas occur in up to 80% of patients with TSC and consist of smooth muscle cells, fibrous tissue, adipocytes, and abnormally formed thick-walled vascular channels (1, 20). Although malignant progression of angiomyolipomas is rare, these lesions can grow, leading to renal insufficiency and/or death from hemorrhage. It also has been shown that renal carcinogenesis in $Tsc2^{+/-}$ mice is greatly reduced when IFN-γ levels are increased by an IFN-γ transgene (21). In addition, total signal transducers and activators of transcription (STAT) 3 levels and pSTAT3 Ser727 and pSTAT3 Tyr705 levels are increased in Tsc2 null neuroepithelial progenitor cells compared with controls (22). Additionally, smooth muscle cell proliferation and growth are reduced by up to 70% when they are cocultured with IFN-γ-transduced endothelial cells (23), and IFN-γ treatment inhibits airway smooth muscle cell proliferation by blocking transition from the G_1 to S phase (24). IFN-γ is a pleiotropic cytokine involved in antiproliferative and antiviral responses, immune surveillance, and tumor suppression (25, 26). Biological responses to IFN-γ are mediated mainly by the regulation of gene expression by the Jak-STAT1 pathway (25, 26).

We explore the effects of Tsc1 or Tsc2 deletion on the secretion of IFN-γ and signaling through the IFN-γ-Jak-STAT pathway in cultured cell lines and Tsc mouse models. We demonstrate that IFN-γ is reduced in Tsc1 and Tsc2 null cell lines and tumors, and IFN-γ treatment selectively inhibits proliferation of cells lacking either Tsc1 or Tsc2 and causes apoptosis. We also show that inhibition of mTOR activation by rapamycin in these cells induces IFN-γ secretion. Finally, we demonstrate that a combination treatment of IFN-γ and rapamycin has synergistic effects in the induction of apoptosis in cells lacking Tsc1 or Tsc2.

MATERIALS AND METHODS

Reagents and Antibodies. Reagents were obtained from the following sources: rapamycin, Cell Signaling Technology (Beverly, MA); IFN-γ, R&D Systems (Minneapolis, MN); DMEM and FCS, Mediatech, Inc. (Herndon, VA); IFN-γ ELISA kit, BioSource International (Camarillo, CA); VEGF ELISA kit, Oncogene Research Products (Boston, MA); ImmunoCruz Staining kit, Santa Cruz Biotechnology (Santa Cruz, CA); and FlowTACS FITC apoptotic kit, Trevigen Inc. (Gaithersburg, MD).

Antibodies against the following proteins were obtained from the following sources: bcl-2, bax, proliferating cell nuclear antigen, tuberin, actin, IFN-γ-Rα, IFN-γ-Rβ, Jak1, Jak2, extracellular signal-regulated kinase, S6K, and AKT, Santa Cruz Biotechnology; pS6 (Ser235/236), pS6 (Ser240/244), pSTAT1 Tyr701, STAT1, pSTAT3 Tyr705, and caspase-1 and -9, Cell Signaling Technology; pSTAT1 Ser727, Upstate Signaling (Lake Placid, NY); and STAT3, BD Biosciences (Palo Alto, CA). An antihamartin antibody, HM4, was described previously (7).

MEF Cell Culture. Immortalized mouse embryo fibroblast (MEF) cell lines that had genotype $Tsc1^{-/-}$ prepared by the mouse fibroblast cell technique and $Tsc2^{-/-}$ $TP53^{-/-}$ MEF lines were prepared and cultured as described previously (7, 27). Littermate controls for these lines were used for comparison. For the Tsc2 null lines, the controls had the genotype $TP53^{-/-}$. For simplicity, we refer to $Tsc2^{-/-}$ $TP53^{-/-}$ cells as $Tsc2^{-/-}$,

Received 11/17/03; revised 2/16/04; accepted 2/24/04.

Grant support: LAM Foundation, the Rothberg Fund, and NIH NINDS.

The costs of publication of this article were defrayed in part by the payment of page charges. This article must therefore be hereby marked *advertisement* in accordance with 18 U.S.C. Section 1734 solely to indicate this fact.

Requests for reprints: David J. Kwiatkowski, Brigham and Women's Hospital, Hematology Division, Department of Medicine, CHNRB6-0216, 75 Francis St., Boston, MA 02115. Phone: 617-355-9005; Fax: 617-355-9016; E-mail: dk@rics.bwh.harvard.edu.

their *TP53*$^{-/-}$ controls as *Tsc*$^{+/+}$, mouse fibroblast *Tsc1*$^{-/-}$ cells as *Tsc1*$^{-/-}$, and their controls as *Tsc*$^{+/+}$.

Generation of Retroviral Vectors and Revertant Cells. PT67, pLXIN, pIREShyg3, and hygromycin B were purchased from Clontech (Palo Alto, CA). A DNA fragment containing internal ribosomal entry site (IRES) and hygromycin B phosphotransferase gene was PCR amplified from pIREShyg3 and inserted into pLXIN, replacing the IRES and neomycin resistance gene. The human TSC2 cDNA then was subcloned into the pIREShyg retroviral vector. A construct containing a TSC2 mutation was generated using the QuickChange site-directed mutagenesis kit (Stratagene, La Jolla, CA). Plasmids were transfected with Lipofectamine 2000 (Invitrogen, Carlsbad, CA) into the retroviral packaging cell line PT67. Filtered supernatants containing virus were used to infect *Tsc2*$^{-/-}$ MEF cells, followed by selection with 100 μg/ml hygromycin B.

Cell Growth Assays. For cell growth assays, cells were plated at 1×10^5 cells/well of a six-well plate in DMEM with 10% FCS. After 6 h, the media were replaced with DMEM alone for up to 48 h. Combinations of rapamycin, IFN-γ, and other agents then were added for the specified intervals. Cells were counted using a hemacytometer, and 0.4% trypan blue was used to distinguish viable from dead or dying cells.

IFN-γ and VEGF Measurements. IFN-γ levels from cell cultures and serum were determined by ELISA using a mouse IFN-γ kit (Biosource International) following instructions supplied by the manufacturer. VEGF measurements also were determined by ELISA kit specific for mouse VEGF (Oncogene Research Products). For VEGF measurements, 50 μl undiluted cell culture media were added to the assay.

Immunohistochemistry and Immunoblotting. Immunohistochemistry was performed on 5-μm paraffin-embedded tissue sections. They were deparaffinized in xylene and rehydrated in an ethanol/water series. Sections were stained by the peroxidase method (goat ImmunoCruz staining kits, Santa Cruz Biotechnology) using primary antibody against IFN-γ (Santa Cruz Biotechnology) and were counterstained with hematoxylin. Negative control immunohistochemical procedures were conducted on adjacent tissue sections, including replacement of the primary antibody with normal IgG.

For Western blot analysis, cells, liver hemangioma, normal liver, kidney cystadenomas, and normal kidney tissues were washed with cold PBS and lysed on ice with lysis buffer [60 mM Tris-HCL (pH 6.8), 2% SDS, 10% glycerol, and 100 mM DTT]. Aliquots containing equal amounts of proteins were denatured at 100°C for 5 min, separated by SDS-PAGE, and then transferred onto nitrocellulose membranes (Bio-Rad, Hercules, CA). After probing with antibodies and rinsing, membranes were developed with horseradish peroxidase-conjugated antimouse, antigoat, or antirabbit secondary antibodies (Santa Cruz Biotechnology) using enhanced chemiluminescence (Pierce, Rockford, IL). All of the immunoblots shown in one row of a figure are from the same gel blot exposure.

Apoptosis Assays. Apoptosis was determined using FlowTACS FITC kit (Trevigen) following the manufacturer's instructions, which are based on 3′ end labeling of DNA fragments using FITC-conjugated nucleotides. Apoptosis was determined by analysis of the amount of fluorescence per cell using flow cytometry (fluorescence-activated cell sorter caliber flow cytometry, B&D Biosciences, San Jose, CA). Ten thousand events were acquired per sample.

RESULTS

IFN-γ Expression in Tsc-Associated Lesions. We have described Tsc mouse models that have been developed by gene targeting and inactivation of *Tsc1* and *Tsc2* (7, 28). *Tsc1*$^{+/-}$ and *Tsc2*$^{+/-}$ mice commonly develop liver hemangiomas, renal cystadenomas, and, more rarely, angiosarcomas. IFN-γ expression in *Tsc1*$^{+/-}$ and *Tsc2*$^{+/-}$ mouse tumors was examined by immunohistochemistry and immunoblot analyses. IFN-γ staining was absent completely in liver hemangioma and kidney cystadenomas of *Tsc1*$^{+/-}$ and *Tsc2*$^{+/-}$ mice compared with surrounding normal and wild-type tissues (Fig. 1, *A–C*). Similarly, major differences in IFN-γ content were seen in extracts obtained from these tumors (Fig. 1*D*).

IFN-γ Secretion by Tsc Null Cells. The above results suggested that cells lacking Tsc1 or Tsc2 might have reduced secretion of IFN-γ.

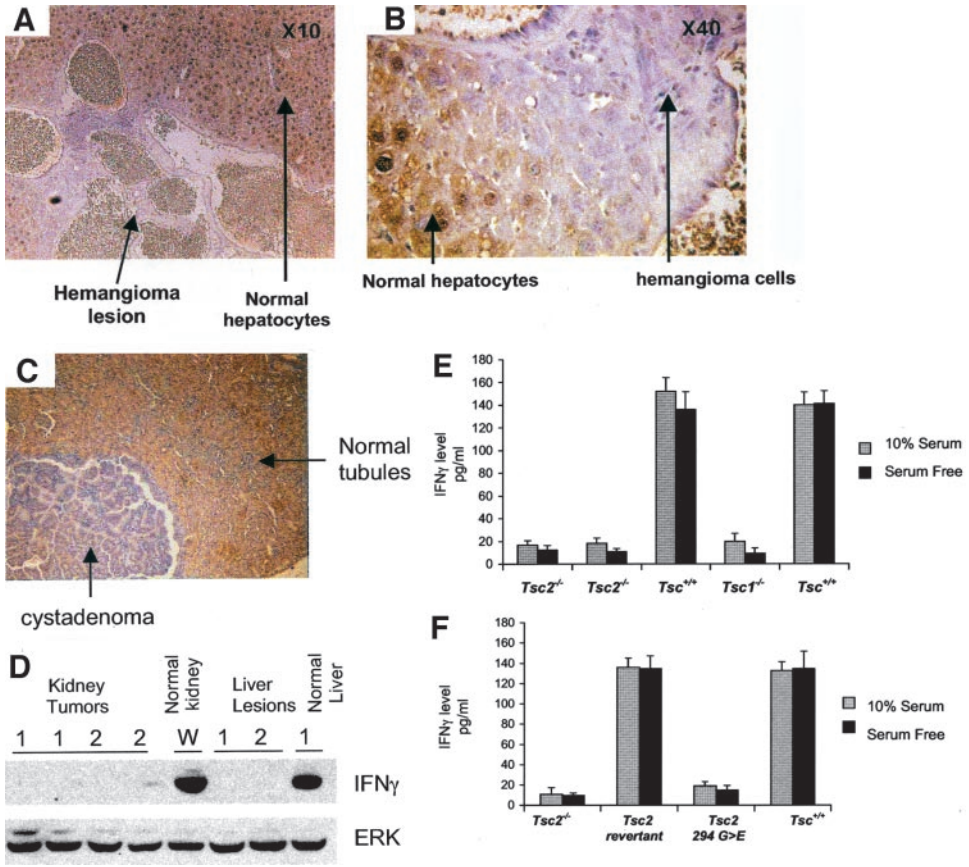

Fig. 1. IFN-γ expression in Tsc mouse lesions and cell lines. *A–C*, immunohistochemistry analysis of IFN-γ showing expression in normal tissues but not in a *Tsc1*$^{+/-}$ liver hemangioma (*A* and *B*) or a *Tsc2*$^{+/-}$ kidney tumor (*C*). *D*, immunoblot analysis of IFN-γ expression in Tsc kidney tumors and liver hemangiomas. Note absence of IFN-γ in the lesions (*1* denotes *Tsc1*$^{+/-}$, *2* denotes *Tsc2*$^{+/-}$, and *W* denotes wild type). *E*, IFN-γ secretion in *Tsc1*$^{-/-}$ and *Tsc2*$^{-/-}$ fibroblast cell lines is reduced compared with control cell lines as assessed by ELISA 24 h after plating. *F*, similar assay as *E* showing IFN-γ secretion was restored in a Tsc2 revertant but not in a Tsc2 mutant (294 G→E) revertant cell line.

We examined IFN-γ secretion levels in a set of *Tsc1*$^{-/-}$, *Tsc2*$^{-/-}$, and control (denoted *Tsc*$^{+/+}$) MEF cell lines (see "Materials and Methods"). We found that IFN-γ levels in conditioned media derived from *Tsc1*$^{-/-}$and *Tsc2*$^{-/-}$ cells were reduced dramatically when compared with wild-type cells (Fig. 1*E*). To confirm that decreased production of IFN-γ was a direct result of loss of either Tsc gene product, we examined IFN-γ levels in conditioned media from *Tsc2*$^{-/-}$ cells transfected to express normal human TSC2, and a patient-derived TSC2 missense mutation (294 G→E). We found that IFN-γ levels were increased significantly in media from the Tsc2 revertant cells but not in that from Tsc2 mutant cells (Fig. 1*F*).

Because tumors developing in Tsc mouse models are deficient in Tsc1 or Tsc2, we also investigated the possibility that IFN-γ levels might be reduced in these mice. IFN-γ serum levels were reduced significantly in *Tsc1*$^{+/-}$ (range, 19–56 pg/ml) and *Tsc2*$^{+/-}$ (range, 8–34 pg/ml) mice compared with wild-type controls of similar age (range, 75–85 pg/ml; $P = 0.031$ and 0.019 for the two comparisons, respectively; Table 1). Necropsy analysis showed that *Tsc1*$^{+/-}$ and *Tsc2*$^{+/-}$ mice with low serum levels of IFN-γ always had either grossly visible liver hemangiomas or multiple grossly visible renal cystadenomas, or both (Table 1).

IFN-γ Treatment Reduces Tsc Null Cell Proliferation and VEGF Production. Because IFN-γ has antiproliferative effects on many cell types and because IFN-γ production is reduced in Tsc null cells, we examined the effect of IFN-γ treatment on growth of *Tsc1*$^{-/-}$, *Tsc2*$^{-/-}$, and wild-type control cell lines. IFN-γ treatment reduced the number of viable *Tsc1*$^{-/-}$and *Tsc2*$^{-/-}$cells in a time- and dose-dependent manner, whereas wild-type control cell lines showed an opposite proliferative response to IFN-γ treatment (Fig. 2*A*). To confirm these observations, we examined Tsc2 revertant and mutant transfected cells under similar conditions. IFN-γ reduced the number of cells expressing the Tsc2 mutant cDNA (294 G→E), whereas Tsc2 revertant cells showed a proliferative response to IFN-γ (Fig. 2*B*).

We have demonstrated previously that high levels of VEGF are secreted by Tsc null cells and that serum levels of VEGF are increased in *Tsc1*$^{+/-}$ and *Tsc2*$^{+/-}$ mice (16). IFN-γ treatment caused a dose- and time-dependent decrease in VEGF secretion by *Tsc1*$^{-/-}$ and *Tsc2*$^{-/-}$ cells (Fig. 2*C*). In contrast, wild-type control cell lines showed an increase of VEGF secretion in response to IFN-γ (Fig. 2*C*). The decrease in VEGF secretion by the null cell lines may be caused largely by the reduction in cell numbers induced by IFN-γ but also may reflect a specific effect of IFN-γ treatment on VEGF production.

IFN-γ Treatment Induces Apoptosis in Tsc Null Cell Lines. To explore the mechanism of the reduction in cell number in Tsc null cells in response to IFN-γ treatment, we looked for evidence of apoptosis. DNA fragmentation indicative of apoptosis-associated DNAase activity in IFN-γ treated cells was studied using a flow cytometry assay. DNA fragmentation was much higher in IFN-γ-treated Tsc null cells when compared with untreated Tsc null or wild-type cells (Fig. 3, *A–D*). To understand the cause of IFN-γ-induced apoptosis by Tsc null cells, the expression of several proliferative and apoptotic proteins was assessed by immunoblot analysis. Proliferating cell nuclear antigen expression (reflecting enhanced proliferation) and bcl-2 (antiapoptotic protein) expression were increased

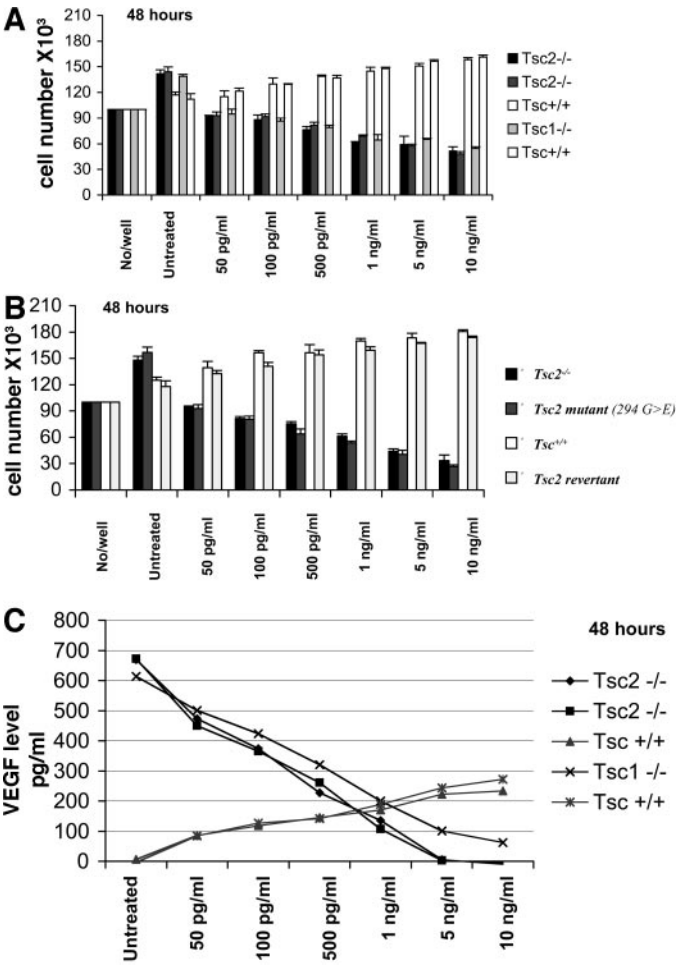

Fig. 2. Growth and vascular endothelial growth factor (*VEGF*) secretion by Tsc lines in response to IFN-γ treatment. *A*, IFN-γ treatment for 48 h reduced cell number in *Tsc1*$^{-/-}$ and *Tsc2*$^{-/-}$ cells in a time- and dose-dependent manner. A total of 100×10^3 cells were plated per well in six-well plates. Observations reflect an average of three different experiments performed in triplicate; bars, SD. *B*, identical to *A*, performed on Tsc2 revertant and mutant cell lines. *C*, IFN-γ treatment for 48 h reduced VEGF secretion of *Tsc1*$^{-/-}$ and *Tsc2*$^{-/-}$ cells but increased it in control cells.

Table 1 *Serum level of IFN-γ (pg/ml) and pathologic findings in Tsc1*$^{+/-}$, *Tsc2*$^{+/-}$, *and wild-type control mice*

Genotype	Strain	Age (months)	Sex	Liver hemangioma	Kidney cystadenoma	IFN-γ level (pg/ml)
Tsc1$^{+/-}$	129sv	16	Male	Small one lobe	None	43
	129sv	16	Male	Massive multilobar	6	23
	129sv	16	Male	Small multilobar	1	25
	129sv	16	Male	Small multilobar	2	24
	129sv	16	Male	Small multilobar	1	20
	129sv	16	Male	Massive multilobar	1	17
	129sv	16	Male	Small multilobar	6	19
	129sv	16	Male	None	3	56
Tsc2$^{+/-}$	129sv/B6	15	Female	Massive multilobar	5	8
	129sv/B6	15	Male	Massive one lobe	7	16
	129sv/B6	15	Male	None	7	34
Tsc$^{+/+}$	129sv	13	Male	None	None	75
	129sv	13	Male	None	None	85
	129sv	13	Male	None	None	77

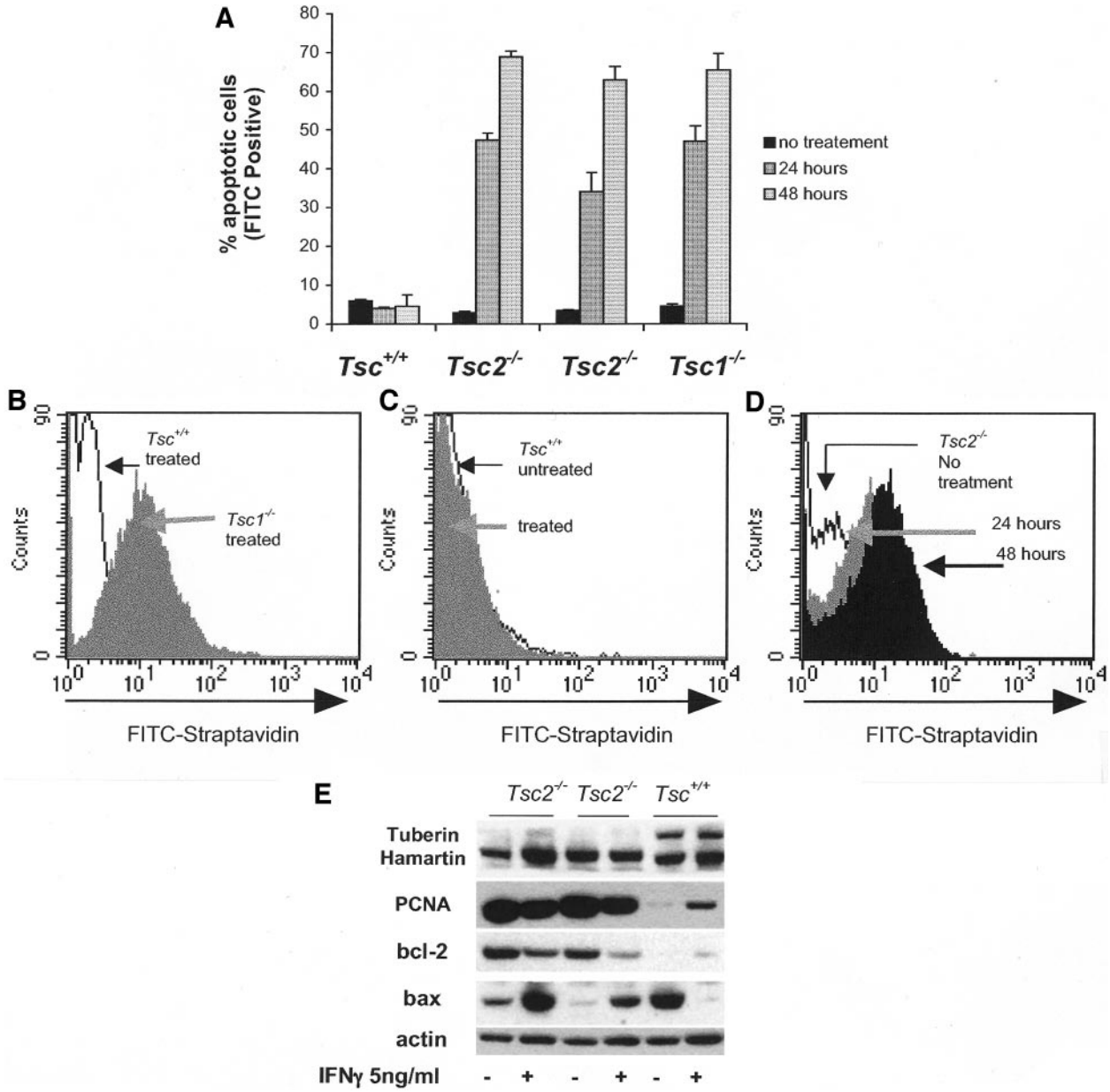

Fig. 3. IFN-γ treatment induces apoptosis in *Tsc1*$^{-/-}$ and *Tsc2*$^{-/-}$ cells. *A–D*, induction of apoptosis by IFN-γ in *Tsc1*$^{-/-}$ and *Tsc2*$^{-/-}$ cells but not in wild-type cells. *A*, the percentage of cells showing DNA fragmentation as assessed by FITC staining at 24 h and 48 h after addition of 5 ng/ml IFN-γ. *B–D*, fluorescence-activated cell sorter analysis showing histograms of cell populations at various time points following IFN-γ treatment. *B*, *Tsc1*$^{-/-}$ and control wild-type cell lines 24 h after IFN-γ treatment. *C*, control line with or without IFN-γ for 24 h. *D*, *Tsc2*$^{-/-}$ cell line at time 0, 24, and 48 h after IFN-γ treatment. *E*, immunoblot analysis of two different *Tsc2*$^{-/-}$ lines and a control line treated with or without 5 ng/ml IFN-γ for 48 h, showing a reduction in proliferating cell nuclear antigen and antiapoptotic gene bcl-2 in *Tsc2*$^{-/-}$-treated cells compared with untreated *Tsc2*$^{-/-}$ and Tsc wild-type cells. Expression of the proapoptotic gene bax increased in response to IFN-γ treatment.

in untreated Tsc2 null cells compared with wild-type cells, whereas bax (proapoptotic protein) expression was reduced in Tsc null cells. In response to 24-h IFN-γ treatment, bcl-2 expression decreased, whereas bax expression increased in Tsc null cells; in contrast, bax expression decreased in response to IFN-γ treatment in wild-type control cells (Fig. 3*E*).

Furthermore, IFN-γ treatment induced caspase-1 and -9 expression in Tsc null cells in contrast to wild-type cells (see below; Fig. 4*E*). These results suggest that these differences in bcl-2/bax and caspase-1 and -9 expression in Tsc null cells contribute to their apoptotic response to IFN-γ.

IFN-γ-STAT1 Signaling *in Vivo* and *in Vitro*. IFN-γ exerts its effects on cells by interacting with its receptors (IFN-γ-Rα and IFN-γ-Rβ), which induce activation of the receptor-associated Janus kinases Jak1 and Jak2, leading to phosphorylation of STAT1 on tyrosine 701 (26). STAT1 also is phosphorylated on serine 727 in response to IFN-γ in many cell types, and this enhances its transcriptional activity (26). To explore the molecular basis of the differential effects of IFN-γ treatment on Tsc null cells, we examined the expression and activation of proteins in the Jak-STAT1 signaling pathway in *Tsc2*$^{-/-}$ and wild-type cells (Fig. 5*A*). IFN-γ-Rα and -Rβ and Jak1 expression levels were similar in both sets of cells. However, Jak2 expression levels were decreased mildly in Tsc null cells (three of four cases) compared with wild-type cells. Additionally, STAT1 levels were increased dramatically in Tsc1 and Tsc2 null cells compared with wild-type cells, and pSTAT1 Ser727 was seen at significant levels in Tsc1 or Tsc2 null cells alone without stimulation (Fig. 5*A*). We also examined this pathway in tumors developing in *Tsc1*$^{+/-}$ and

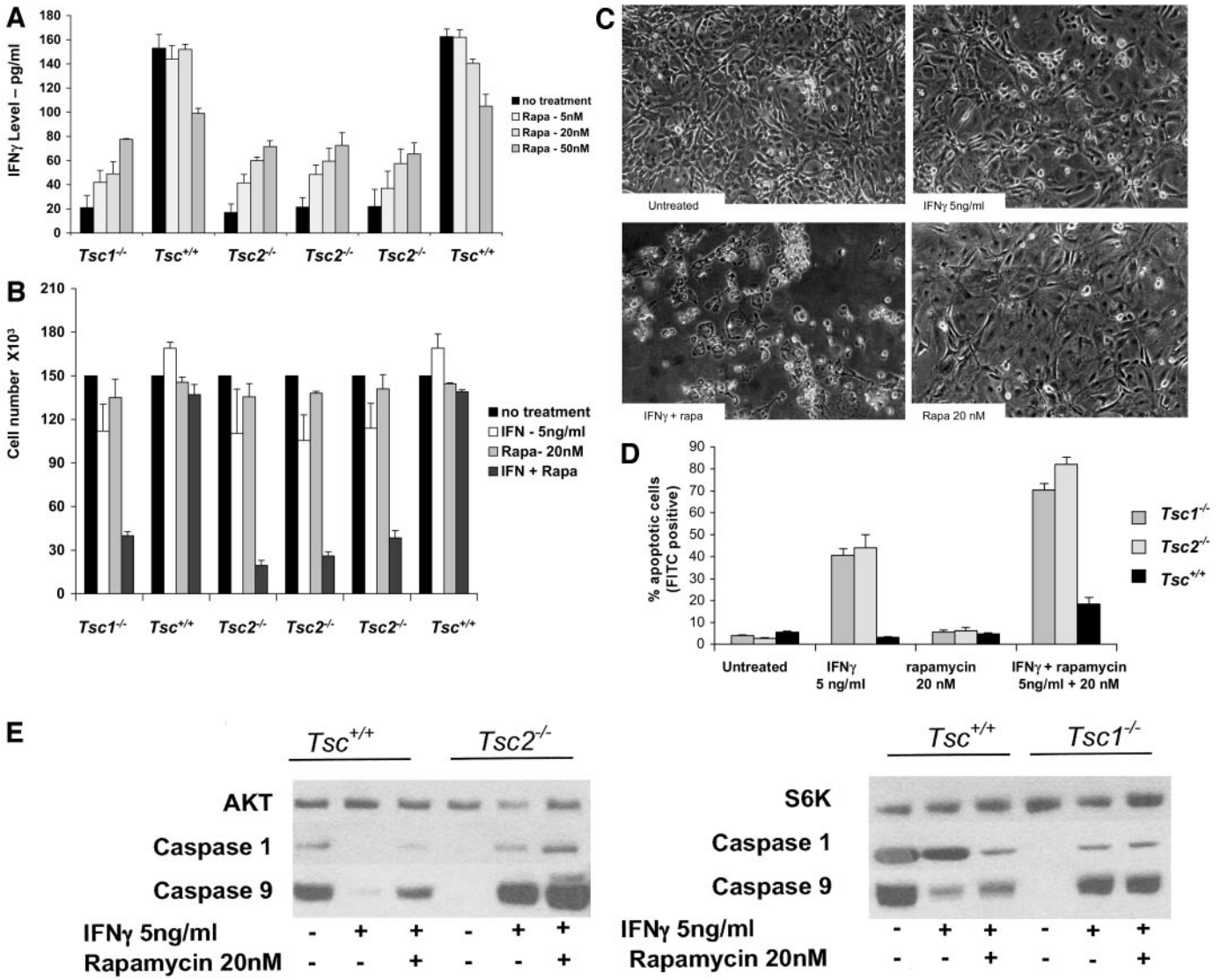

Fig. 4. Synergistic effect of IFN-γ-rapamycin on cell survival and apoptosis of $Tsc1^{-/-}$ and $Tsc2^{-/-}$ cell lines. *A*, IFN-γ secretion assessed by ELISA in $Tsc1^{-/-}$ and $Tsc2^{-/-}$ fibroblast cell lines following treatment with rapamycin for 24 h. IFN-γ levels increase in $Tsc1^{-/-}$ and $Tsc2^{-/-}$ cell lines in a dose-dependent manner. *B*, a combination of 5 ng/ml IFN-γ and 20 nM rapamycin for 24 h dramatically reduced the number of $Tsc1^{-/-}$ and $Tsc2^{-/-}$ cells compared with Tsc null cells treated with either IFN-γ or rapamycin only. *C*, phase contrast views of the effect of combined IFN-γ-rapamycin treatment on $Tsc2^{-/-}$ cells. *D*, the percentage of cells showing DNA fragmentation 24 h after initiation of treatment. *E*, IFN-γ alone and combined IFN-γ-rapamycin treatment induced caspase-1 and -9 expression in Tsc null cells in contrast to wild-type controls.

$Tsc2^{+/-}$ mice and found similar results. INF-Rα, INF-Rβ, Jak1, and Jak2 levels were not different in tumors compared with control tissues (Fig. 5*B*). However, STAT1 and pSTAT1 Ser727 were seen only in the tumor extracts but not in normal kidney and liver tissues of $Tsc1^{+/-}$ and $Tsc2^{+/-}$ mice (Fig. 5*B*).

Because loss of either *TSC* gene leads to unregulated activation of mTOR, we also examined the effect of short-term rapamycin treatment (2 h) on STAT1 in $Tsc1^{-/-}$ and $Tsc2^{-/-}$ and wild-type cells (7–11). Rapamycin reduced levels of pSTAT1 Ser727 in $Tsc1^{-/-}$ and $Tsc2^{-/-}$ cells, whereas STAT1 levels remained stable (Fig. 5*C*). In contrast, short-term rapamycin treatment increased pSTAT1 Ser727 levels in control cells. These data are consistent with STAT1 being phosphorylated at Ser727 by mTOR in Tsc2 null cells.

STAT3 Is Activated in Tsc Null Cells. Because STAT3 has effects in many cell types that counterbalance those of STAT1 and because we previously had seen STAT3 phosphorylation in Tsc2 null neuroepithelial precursor cells (22), we also examined STAT3 expression and activation. We found that the expression of STAT3 was similar in $Tsc1^{-/-}$, $Tsc2^{-/-}$, and control cells. However, levels of pSTAT3 Tyr705 were increased markedly in $Tsc1^{-/-}$ and $Tsc2^{-/-}$ cells compared with controls (Fig. 5*D*). IFN-γ treatment for 24 h reduced pSTAT3 Tyr705 levels in $Tsc1^{-/-}$ and $Tsc2^{-/-}$ cells, which was enhanced by cotreatment with rapamycin. In contrast, IFN-γ treatment led to phosphorylation of STAT3 at Tyr705 in control cells (Fig. 4*D*), which might explain the proliferative effect of IFN-γ on wild-type control cell lines. The major reduction in pSTAT3 Tyr705 and the activation of STAT1 Tyr701 that occurs in Tsc1 or Tsc2 null cells in response to IFN-γ likely contribute to their apoptotic response to IFN-γ.

Rapamycin Stimulates IFN-γ Secretion *in Vitro*. We then investigated the effect of rapamycin on IFN-γ production by Tsc null cell lines. In $Tsc1^{-/-}$ and $Tsc2^{-/-}$ cells, we observed that rapamycin induced IFN-γ secretion in a dose-dependent manner (Fig. 4*A*). In contrast, although low doses of rapamycin (5–20 nM) had little effect, 50 nM rapamycin inhibited IFN-γ secretion in wild-type cells (Fig. 4*A*). These results suggest that mTOR activation in Tsc null cells leads to suppression of IFN-γ secretion, and that when mTOR is inhibited by rapamycin, IFN-γ production resumes.

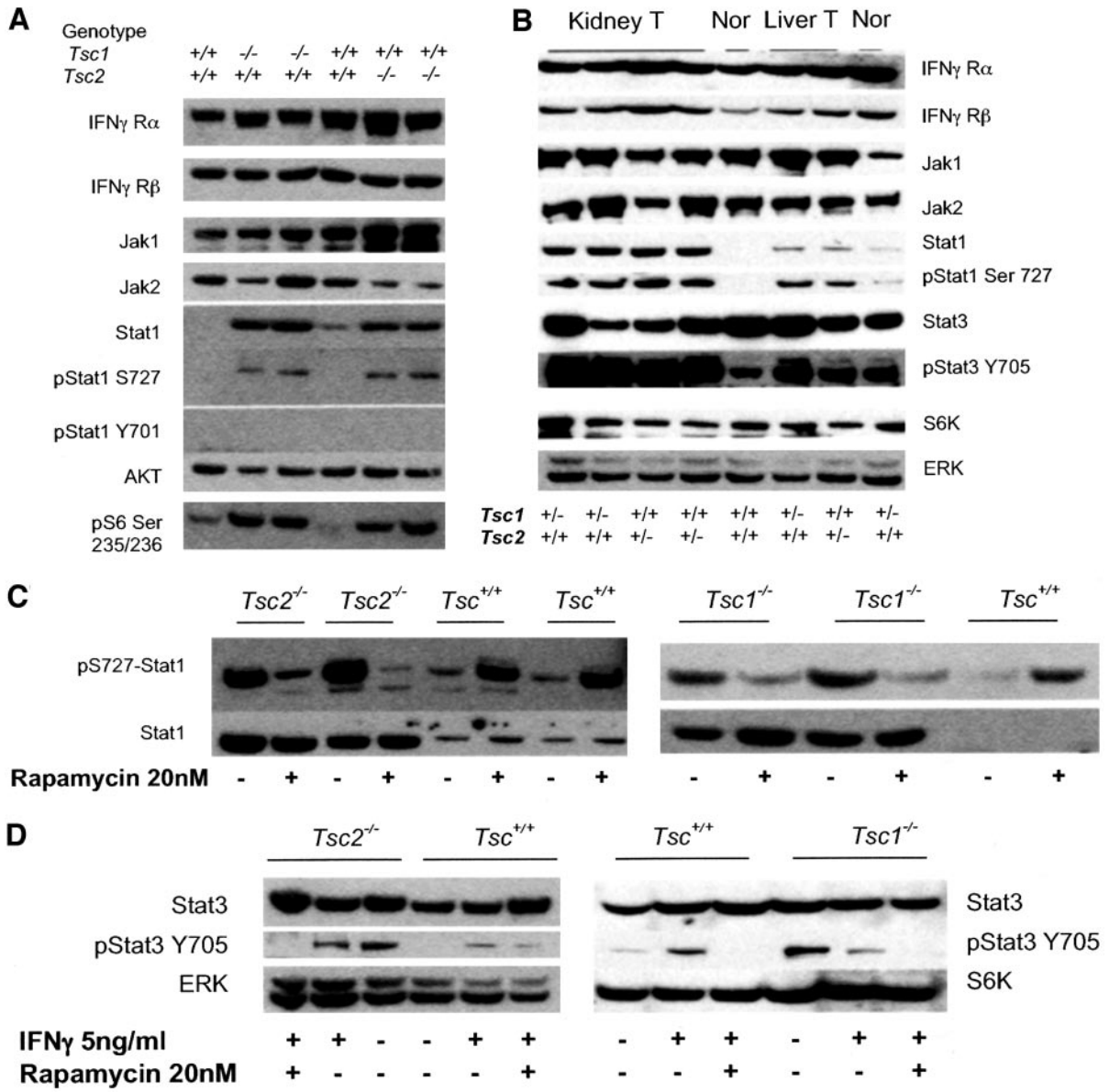

Fig. 5. IFN-γ-Jak-signal transducers and activators of transcription (*STAT*) 1 pathway in Tsc null and control cell lines. *A*, immunoblot analysis shows that expression of IFN-γ-Rα, IFN-γ-R*β*, and Jak1 is similar in two Tsc2 null, two Tsc1 null, and two control cell lines. Jak2 expression is slightly reduced in three of four Tsc null cells. STAT1 expression is increased and pSTAT1 Ser727 is present in *Tsc* null cells but not in control cells. No pSTAT1 Tyr701 was seen in these cell lines. *B*, immunoblot analysis of Tsc mouse kidney and liver tumors (*T*, tumor; *Nor*, normal). Note increased STAT1, pSTAT1 Ser727, and pSTAT3 Tyr705 in Tsc tumors as compared with normal tissues. *C*, rapamycin effects on STAT1. Twenty nM of rapamycin for 2 h reduced pSTAT1 Ser727 levels in Tsc2 null cells and Tsc1 null cells, whereas it increased levels in control cell lines. *D*, Treatment of 5 ng/ml IFN-γ for 24 h generates pSTAT3 Tyr705 in control wild-type cells, while reducing levels of the same in $Tsc1^{-/-}$ and $Tsc2^{-/-}$ cell lines. Five ng/ml IFN-γ and 20 nM rapamycin for 12 h eliminated pSTAT3 Tyr705 in $Tsc1^{-/-}$ and $Tsc2^{-/-}$ and control cell lines.

Synergism between IFN-γ and Rapamycin on Tsc1/Tsc2 Null Cells. Rapamycin reduces the proliferation of $Tsc2^{-/-}$ and $Tsc1^{-/-}$ cell lines (27). Therefore, we explored combined treatment with IFN-γ and rapamycin on these cell lines. A combination of 5 ng/ml IFN-γ and 20 nM rapamycin had markedly synergistic effects in reducing cell numbers compared with either treatment given individually (Fig. 4, *B* and *C*). The combination of IFN-γ and rapamycin had minimal effects on wild-type cells. Furthermore, the combination of IFN-γ and rapamycin induced apoptosis to a major extent in $Tsc1^{-/-}$ and $Tsc2^{-/-}$ cells, as assessed by fluorescence-activated cell sorter analysis, in contrast to wild-type cells (Fig. 4*D*). Moreover, the expression of caspase-1 and -9 was induced in $Tsc1^{-/-}$ and $Tsc2^{-/-}$ cells treated with combined IFN-γ and rapamycin (Fig. 4*E*).

We also examined the effect of combined IFN-γ and rapamycin treatment on STAT1 and STAT3 levels and activation in null and wild-type cells. The combination reduced pSTAT1 Ser727 levels to a modest extent (Fig. 6*A*) and sharply reduced pSTAT3 Tyr705 levels in $Tsc2^{-/-}$ cells (Fig. 5*D* and Fig. 6*B*). IFN-γ alone led to a marked increase in pSTAT1 Tyr701 levels in both types of cells, whereas combined IFN-γ-rapamycin treatment led to high levels of pSTAT1 Tyr701 in the null cells only (Fig. 6, *A* and *B*).

We confirmed the specificity of these findings by analysis of revertant TSC2-transfected and nonrevertant TSC2 mutant-transfected cell lines. pSTAT1 Tyr701 and pSTAT1 Ser727 levels were much higher in IFN-γ-rapamycin-treated $Tsc2^{-/-}$ and mutant revertant cells than in revertant cells. pSTAT3 Tyr705 levels were high in control and IFN-γ-treated $Tsc2^{-/-}$ and mutant revertant lines but were abolished by rapamycin or IFN-γ-rapamycin treatment. Bcl-2 expression also was abolished, whereas bax expression was induced by IFN-γ-rapamycin treatment of $Tsc2^{-/-}$ and mutant revertant cells.

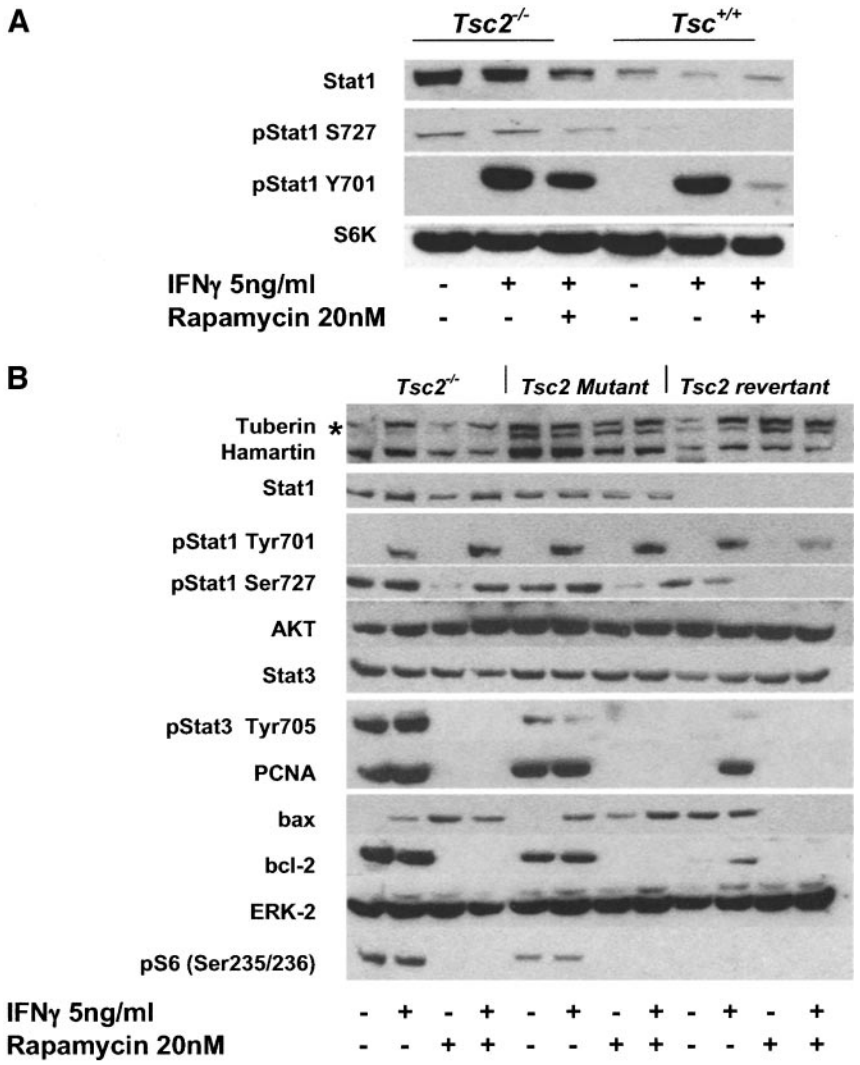

Fig. 6. Analysis of Jak-signal transducers and activators of transcription (STAT) signaling in response to IFN-γ and rapamycin treatment. Immunoblot analyses of *Tsc2*$^{-/-}$ and a control cell line (*A*) or *Tsc2*$^{-/-}$, Tsc2 mutant, and Tsc2 revertant cell lines (*B*) following treatment with 5 ng/ml IFN-γ, 20 nM rapamycin, or a combination of 5 ng/ml IFN-γ and 20 nM rapamycin for 12 h. Note that a combination of IFN-γ-rapamycin leads to increased pSTAT1 Tyr701 levels, persistent pSTAT1 Ser727 levels, and induction of bax with elimination of bcl-2 levels in Tsc null cells and mutant cells but not in revertant cells. Rapamycin effect in Tsc2 null and mutant cells is confirmed by the reduction in pS6 Ser235/236. *Nonspecific band.

DISCUSSION

The canonical IFN-Jak-STAT signaling pathway begins with receptors IFN-γ-Rα and IFN-γ-Rβ, which reside in the cell membrane. On binding to IFN-γ, these receptors form aggregates, bringing the Jak1 and Jak2 kinases, which normally are bound to individual receptors, in close proximity, so that they can phosphorylate each other. The activated phosphorylated Jaks then phosphorylate IFN-γ-Rα at Tyr440, creating a binding site for the SH2 domain of STAT1 and leading to Jak phosphorylation of STAT1 at Tyr701. pSTAT1 Tyr701 dissociates from the IFN-γ-R, dimerizes through reciprocal pSTAT1 Tyr701-SH2 domain interactions, and translocates to the nucleus to bind to γ-activated sequence elements in the promoters of IFN-γ-responsive genes, leading to transcriptional effects (26).

This canonical pathway has been recognized for some time to be influenced by a variety of other cytokines and their receptors (so-called cross-talk) and a number of proteins that are negative regulators of Jak-STAT signaling, including cytoplasmic phosphatases, suppressor of cytokine signaling proteins that bind to activation sites on receptors and Jaks, and proteins that inhibit activated STATS that reside in the nucleus and bind to and sequester phosphorylated STATS (26).

Phosphorylation of STAT1 at Ser727 also has major effects on its transcriptional activity (29, 30). The Ser727A mutant STAT1 has only ~20% of the transcriptional activity of wild-type STAT1 (31). Phosphorylation of STAT1 at Ser727 has been shown to occur in response to multiple stimuli, including IFN-γ; IFN-α; UV irradiation; platelet-derived growth factor; interleukins 1, 2, and 12; and tumor necrosis factor α (30). Phosphorylation at Ser727 in response to IFN-γ has been shown to depend on phosphatidylinositol 3′-kinase and Akt, functional Jak1 and Jak2, and an intact STAT1 recruitment site on IFN-R (31).

We have shown that there is a major decrease of IFN-γ levels and increase of total STAT1 level and constitutive phosphorylation of STAT1 Ser727 and STAT3 Tyr705 in MEF cell lines lacking either Tsc1 or Tsc2, and in kidney and liver tumors from *Tsc1*$^{+/-}$ and *Tsc2*$^{+/-}$ mice. The reduction of IFN-γ levels is reversed by rapamycin treatment, suggesting that mTOR activation is responsible for the decrease in IFN-γ levels. In addition, the increase in pSTAT1 Ser727 is sensitive to rapamycin treatment and, given previous observations, suggests that mTOR or a kinase downstream of mTOR is directly responsible for phosphorylation at this site. The observations provide strong support for the concept that Akt does not directly phosphorylate STAT1 because Akt is strongly inactivated even in response to serum stimulation in cells lacking Tsc1 or Tsc2 (27). Nonetheless, the occurrence of this phosphorylated STAT1 form is somewhat paradoxical given previous work indicating the necessity for recruitment of STAT1 to the IFN-R for Ser727 phosphorylation to occur (31).

However, this may reflect the highly and persistently active mTOR present in Tsc1 or Tsc2 null cells, which is able to phosphorylate STAT1 without localization to its normal activation site. The presence of Ser727 phosphorylated STAT1 appears to account at least partially for the differential growth response of the Tsc1 or Tsc2 null cells to IFN-γ.

The presence of pSTAT3 Tyr705 in cells lacking Tsc1 or Tsc2 in the absence of IFN-γ stimulation also is unexpected but now has been seen in two different Tsc2 null cell types: MEFs (shown here) and neuroepithelial progenitor cells (22). However, many other growth factors and cytokines can lead to activation of STAT1 and STAT3, and further study will be required to explore the mechanism of this activation. Given the inhibition of phosphatidylinositol 3′-kinase activation and downstream signaling in Tsc2 null cells, it is unlikely that any kinase in the phosphatidylinositol 3′-kinase pathway is responsible for STAT3 Tyr705 phosphorylation (27). In any case, it appears that this persistent activation of STAT3 may contribute to the enhanced growth rate and survival of Tsc1 and Tsc2 null fibroblasts under conditions of serum starvation. Paradoxically, STAT3 activation is reduced somewhat by treatment of the Tsc1 or Tsc2 null cells with IFN-γ alone and is eliminated completely by combined IFN-γ and rapamycin treatment.

Our data show that IFN-γ and rapamycin have synergistic effects in the induction of apoptotic cell death in cells lacking Tsc1 or Tsc2. Short-term treatment with rapamycin does not induce apoptosis in these cells but does rapidly reduce phospho-S6K, pS6, and p4E-BP1 levels (Refs. 10, 27; Fig. 6*B*), cell proliferation (Ref. 27; Fig. 6*B*), and pSTAT1 Ser727 and pSTAT3 Tyr705 levels (Fig. 5*C* and Fig. 6*B*) and also reduces bcl-2 and induces bax expression (Fig. 6*B*). IFN treatment of these cells also reduces bcl-2 and induces bax expression (Fig. 3*E* and Fig. 6*B*) but also induces caspase-1 and -9 expression (Fig. 4*E*) and has the major effect of inducing phosphorylation of STAT1 at Tyr701. Therefore, the rapid high-level induction of apoptosis by combined IFN-γ-rapamycin treatment is likely caused by these combined and synergistic effects in the activation of STAT3 and inhibition of mTOR and STAT1 signaling.

Previous experiments have demonstrated the ability of short-term treatment with rapamycin to reduce proliferation, induce apoptosis, and reduce VEGF production in Tsc mouse and rat models (11, 16). Longer-term treatment to assess response, effectiveness, and tolerability in animal models is ongoing. The current observations suggest that IFN-γ is another treatment that may be beneficial in these model systems and that there may be significant synergy to the combination of rapamycin and IFN-γ. Because both of these agents are available in the clinic and rapamycin trials in patients with TSC are under way,[1] translation of a synergistic effect to a clinical treatment paradigm is possible within the foreseeable future. Appropriate clinical trials will be required to assess this possibility.

ACKNOWLEDGMENTS

We thank Brian Donohue for technical assistance and Dr. Sandra Dabora for providing IFN-γ.

REFERENCES

1. Gomez M, Sampson J, Whittemore V. The tuberous sclerosis complex, 3rd ed. New York: Oxford University Press; 1999.
2. Plank TL, Yeung RS, Henske EP. Hamartin, the product of the tuberous sclerosis 1 (TSC1) gene, interacts with tuberin and appears to be localized to cytoplasmic vesicles. Cancer Res 1998;58:4766–70.
3. van Slegtenhorst M, Nellist M, Nagelkerken B, et al. Interaction between hamartin and tuberin, the TSC1 and TSC2 gene products. Hum Mol Gene 1998;7:1053–7.
4. Dabora SL, Jozwiak S, Franz DN, et al. Mutational analysis in a cohort of 224 tuberous sclerosis patients indicates increased severity of TSC2, compared with TSC1, disease in multiple organs. Am J Hum Genet 2001;68:64–80.
5. Cheadle JP, Reeve MP, Sampson JR, Kwiatkowski DJ. Molecular genetic advances in tuberous sclerosis. Hum Genet 2000;107:97–114.
6. Sepp T, Yates JR, Green AJ. Loss of heterozygosity in tuberous sclerosis hamartomas. J Med Genet 1996;33:962–4.
7. Kwiatkowski DJ, Zhang H, Bandura JL, et al. A mouse model of TSC1 reveals sex-dependent lethality from liver hemangiomas, and up-regulation of p70S6 kinase activity in Tsc1 null cells. Hum Mol Genet 2002;11:525–34.
8. El-Hashemite N, Zhang H, Henske EP, Kwiatkowski DJ. Mutation in TSC2 and activation of mammalian target of rapamycin signalling pathway in renal angiomyolipoma. Lancet 2003;36:1348–9.
9. Goncharova EA, Goncharov DA, Eszterhas A, et al. Tuberin regulates p70 S6 kinase activation and ribosomal protein S6 phosphorylation: a role for the TSC2 tumor suppressor gene in pulmonary lymphangioleiomyomatosis (LAM). J Biol Chem 2002;277:30958–67.
10. Tee AR, Fingar DC, Manning BD, Kwiatkowski DJ, Cantley LC, Blenis J. Tuberous sclerosis complex-1 and -2 gene products function together to inhibit mammalian target of rapamycin (mTOR)-mediated downstream signaling. Proc Natl Acad Sci USA 2002;99:13571–6.
11. Kenerson HL, Aicher LD, True LD, Yeung RS. Activated mammalian target of rapamycin pathway in the pathogenesis of tuberous sclerosis complex renal tumors. Cancer Res 2002;62:5645–50.
12. Inoki K, Li Y, Xu T, Guan KL. Rheb GTPase is a direct target of TSC2 GAP activity and regulates mTOR signaling. Genes Dev 2003;17:1829–34.
13. Tee AR, Manning BD, Roux PP, Cantley LC, Blenis J. Tuberous sclerosis complex gene products, tuberin and hamartin, control mTOR signaling by acting as a GTPase-activating protein complex toward Rheb. Curr Biol 2003;13:1259–68.
14. Garami A, Zwartkruis FJ, Nobukuni T, et al. Insulin activation of Rheb, a mediator of mTOR/S6K/4E-BP signaling, is inhibited by TSC1 and 2. Mol Cell 2003;11:1457–66.
15. Zhang Y, Gao X, Saucedo LJ, Ru B, Edgar BA, Pan D. Rheb is a direct target of the tuberous sclerosis tumour suppressor proteins. Nat Cell Biol 2003;5:578–81.
16. El-Hashemite N, Walker V, Zhang H, Kwiatkowski DJ. Loss of Tsc1 or Tsc2 induces vascular endothelial growth factor production through mammalian target of rapamycin. Cancer Res 2003;63:5173–7.
17. Sehgal SN, Baker H, Vezina C. Rapamycin (AY-22,989), a new antifungal antibiotic. II. Fermentation, isolation and characterization. J Antibiot 1975;28:727–32.
18. Sehgal SN, Camardo JS, Scarola JA, Maida BT. Rapamycin (sirolimus, rapamune). Curr Opin Nephrol Hypertens 1995;4:482–7.
19. Dabora SL, Roberts P, Nieto A, et al. Association between a high-expressing interferon-γ allele and a lower frequency of kidney angiomyolipomas in TSC2 patients. Am J Hum Genet 2002;71:750–8.
20. Karbowniczek M, Yu J, Henske EP. Renal angiomyolipomas from patients with sporadic lymphangiomyomatosis contain both neoplastic and non-neoplastic vascular structures. Am J Pathol 2003;162:491–500.
21. Hino O, Kobayashi T, Mitani H. Prevention of hereditary carcinogenesis. Proc Japan Acad 2002;78:30–2.
22. Onda H, Crino PB, Zhang H, et al. Tsc2 null murine neuroepithelial cells are a model for human tuber giant cells, and show activation of an mTOR pathway. Mol Cell Neurosci 2002;21:561–74.
23. Stopeck AT, Vahedian M, Williams SK. Transfer and expression of the interferon γ gene in human endothelial cells inhibits vascular smooth muscle cell growth in vitro. Cell Transplant 1997;6:1–8.
24. Amrani Y, Tliba O, Choubey D, et al. IFN-γ inhibits human airway smooth muscle cell proliferation by modulating the E2F-1/Rb pathway. Am J Physiol Lung Cell Mol Physiol 2003;284:1063–71.
25. Stark GR, Kerr IM, Williams BR, Silverman RH, Schreiber RD. How cells respond to interferons. Annu Rev Biochem 1998;67:227–64.
26. Ramana CV, Gil MP, Schreiber RD, Stark GR. Stat1-dependent and -independent pathways in IFN-γ-dependent signaling. Trends Immunol 2002;23:96–101.
27. Zhang H, Cicchetti G, Onda H, et al. Loss of Tsc1/Tsc2 activates mTOR and disrupts PI3K-Akt signalling through downregulation of PDGFR. J Clin Invest 2003;112:1223–33.
28. Onda H, Lueck A, Marks PW, Warren HB, Kwiatkowski DJ. Tsc2(+/−) mice develop tumors in multiple sites that express gelsolin and are influenced by genetic background. J Clin Invest 1999;104:687–95.
29. Zhu X, Wen Z, Xu LZ, Darnell JE Jr. Stat1 serine phosphorylation occurs independently of tyrosine phosphorylation and requires an activated Jak2 kinase. Mol Cell Biol 1997;17:6618–23.
30. Decker T, Kovarik P. Serine phosphorylation of STATs. Oncogene 2000;19:2628–37.
31. Bromberg JF, Horvath CM, Wen Z, Schreiber RD, Darnell JE Jr. Transcriptionally active Stat1 is required for the antiproliferative effects of both interferon α and interferon γ. Proc Natl Acad Sci USA 1996;93:7673–8.
32. Nguyen H, Ramana CV, Bayes J, Stark GR. Dependent phosphorylation of STAT1 on serine 727 and activation of gene expression. J Biol Chem 2001;276:33361–8.

[1] http://lam.uc.edu/html/body_RapamycinInterview.html.